

**SUPPLEMENTARY INFORMATION****I. Extended methods section*****Cell derivation and differentiation***

a) mMAPC-U: The two mMAPC-U clones used were derived independently from BM of C57Bl/6 mice with ubiquitous GFP expression (mMAPC-U was generated from C57Bl/6-Tg-eGFP mice, a gift by Dr. I. Weissman, Stanford, USA; mMAPC-U2 was derived from C57Bl/6TgN(act-EGFP)ObsC14-YO1-FM1310 mice, a gift by Dr. M. Okabe, Osaka University, Japan) and were established at the University of Minnesota, Minneapolis, USA. Both mMAPC clones were derived and maintained under low O<sub>2</sub> (5%) and low-serum (2%) conditions, and expressed the pluripotency transcription factor *Oct-4* at similar levels (between 5-10% relative to the expression of murine ES cells compared by Q-RT-PCR)). A full characterization of these clones, as well as a detailed method for their derivation have been recently described(1). Clones mMAPC-2 and mMAPC-1 described in the latter are identical to clones mMAPC-U and mMAPC-U2, respectively. While studies in the moderate ischemia model were done only with the mMAPC-U clone, both murine clones were tested in the severe ischemia model.

b) mBMC: mBMC were freshly isolated immediately before transplantation by flushing the femurs of C57Bl/6-Tg-eGFP mice, depleted of erythrocytes, washed and transplanted.

c) hMAPC-U: hMAPC-U were established at the University of Navarra, Pamplona, Spain, using BM from donors age 18-54. A full characterization of these cells as well as a detailed method for their derivation and culture has been recently described(2). BM samples were obtained after informed consent from the donor according to the guidelines from the Committee on the Use of Human Subjects in Research from the Clínica Universitaria, Pamplona. *Oct-3/4* expression of the cultures was between 0.3-2.2% (relative to the expression of NTERA teratocarcinoma cells compared by Q-RT-PCR). For the studies described here different hMAPC cultures were used simultaneously, and either cells in culture or freshly thawed cells were transplanted with similar results.

d) mMAPC-VP: All mMAPC-VP used in the current studies consisted of an equal mix of EC and SMC progenitors, both differentiated from the mMAPC-U clone. EC and SMC differentiation were performed as described, in the presence of VEGF or TGF- $\beta$ 1, respectively(3, 4). For each differentiated population, a sample was taken aside for quality control by transcriptional analysis for EC or SMC markers, respectively. A representative quality control profile for EC progenitors used in this study and representing average expression of 4 different differentiation sessions is

shown in Figure S3A. The transcriptional profile of the SMC progenitors has been described elsewhere(3, 4).

### ***Mice, surgery and transplantation***

Moderate limb ischemia model: Recipient mice were C57Bl/6 males (12-16 wk of age). Ischemia was induced under anesthesia (100 mg/kg ketamine + 10 mg/kg xylocaine) by ligation of the left and, where indicated, right common femoral arteries. Cells ( $1 \times 10^6$  in total), resuspended in PBS, or PBS alone were injected in equal fractions in the adductor and lower calf region (Figure S1A,B), always on the left side, immediately after ligation .

Severe limb ischemia model: Recipient mice were Balbc/nu:nu males (12-16 wk of age) having a significantly lower spontaneous revascularization ability than C57Bl/6 mice, likely due to strain-related differences in pre-existing collaterals and to their T-cell deficiency(5-8). Ischemia was induced under anesthesia (100 mg/kg ketamine + 10 mg/kg xylocaine) by ligation and transection of the left iliac artery (for laser-doppler studies) or bilateral ligation and transection of the common femoral arteries (for treadmill studies). Cells ( $1 \times 10^6$  in total), resuspended in PBS, or PBS alone were injected as described above (Figure S1A,B), however, cells were injected 5 days after surgery and for treadmill studies both sides were transplanted (each side receiving  $1 \times 10^6$  cells).

As MAPC-U do not express *MHC-I*, and – consequently – are sensitive to natural killer (NK) cell-mediated clearance(9), all mice were injected i.p. with 20  $\mu$ l anti-asialo GM1 antibodies (Wako Chemicals, Osaka, Japan; 20x diluted in PBS) 1-2 hours before transplantation and every 10 days thereafter. These antibodies selectively eliminate NK cells without affecting the macrophage or lymphocyte function(10). Mice were housed in specific pathogen-free conditions and procedures involving animals were performed according to the guidelines of the Institutional Animal Care and Use Committee of the Universities of Minnesota, Navarra and Leuven.

### ***Live imaging and assessment of limb function and blood flow/perfusion***

Live imaging and functional testing: Live imaging was performed using a Leica dissection microscope after anesthetizing the mice with 60 mg/kg Nembutal and gently removing the skin from the hind limbs. Limb function was evaluated by a swim endurance test, as described(11) (moderate model) or a treadmill test (severe model). Briefly, 24 hours before each endurance test mice were trained and conditioned to run on a 4-lane treadmill equipped with an electrical grid system (Columbus Instruments). The endurance test consisted of a progressive acceleration

protocol and was terminated as soon as the mice spent >15 consecutive seconds on the grid. Endurance tests were performed by persons not aware of the treatment condition.

**MRSI:** Muscle energetic status was determined by magnetic resonance spectroscopy/imaging (MRSI) at day 9 using a 9.4 Tesla horizontal magnet (Magnex Scientific) interfaced with a Unity INOVA console (Varian Inc.). Briefly, a multinuclear RF coil probe consisting of a  $^{31}\text{P}$  coil and a  $^1\text{H}$  coil was built for this study. A one-dimensional spectroscopic imaging method was used to acquire multiple in vivo  $^{31}\text{P}$  spectra from the mouse hind limbs. Mice were under isoflurane anesthesia and the body temperature was monitored and maintained at  $\sim 37^\circ\text{C}$  during the MR study. MR data were analyzed using Varian software for obtaining integral of phosphorus creatine (PCr), inorganic phosphate ( $\text{P}_i$ ) and adenosine triphosphate (ATP) signals in  $^{31}\text{P}$  spectra. The metabolite ratios of PCr/ $\text{P}_i$  and PCr/ $\gamma$ -ATP in each  $^{31}\text{P}$  spectrum were determined and used to monitor the high phosphate energy status in the upper and lower limbs. MRSI recordings were performed by persons not aware of the treatment condition of the mice.

**Laser-doppler:** Blood flow was quantified by laser-doppler probing at anatomically fixed locations from below knee-level to foot (Moor Instruments; moderate model), or by whole-limb scanning (Lisca PIM II; severe model) under temperature-controlled conditions, as described(11). Flow measurements were performed by persons not aware of the treatment condition of the mice.

### ***Tissue processing, histology, and microscopy***

**Tissue processing and staining:** At distinct timepoints after ligation, mice were anesthetized with 60 mg/kg Nembutal and perfused with tris-buffered saline (TBS)-adenosine for 2 minutes followed by zinc-paraformaldehyde for 18 minutes. Following dissection, muscles were fixed for an additional 24 hours, divided in two equal pieces and processed for paraffin or OCT embedding. H&E and Sirius red stainings were performed as described(2). For immunohistochemistry and immunofluorescence, a list of primary antibodies is provided as supplementary information (Table S2). Whole muscle viability assays were performed on unfixed tissue slices of  $\sim 2$  mm thickness after staining with tetraphenyltetrazolium chloride (TTC), as described(12).

### **Morphometric analysis:**

***Equipment and software:*** Pictures for morphometric analysis were taken using a Retiga EXi camera (Q Imaging) connected to a Nikon E800 microscope (Nikon) or a Zeiss Axio Imager connected to an Axiocam MRc5 camera (Zeiss) and analysis was performed using Image J, KS300 (Leica) or Openlab 3.1 (Improvision) software. Confocal microscopy was performed on a

Zeiss LSM 510 (Zeiss). All photography and analyses were performed by persons not aware of the treatment condition of the mice.

*Quantification of engraftment:* For each of the animals, the adductor region and gastrocnemius muscles were isolated, fixed and divided in two equal pieces, one for paraffin processing, one for freezing. From each of the two pieces, regions of about 2 mm thickness were serially sectioned, and serial cross-sections (each 70  $\mu\text{m}$  apart) spanning the 2 mm area were screened for the presence of GFP<sup>+</sup> cells (mouse) or human-vimentin<sup>+</sup> cells (human). For the frozen sections, cells were localized by their GFP fluorescence, for the paraffin sections, by staining with an anti-GFP antibody. Cell engraftment was assessed by two methods: first, the cell patch sizes were determined for individual cross-sections in two dimensions; second, cell density (expressed as number of cells/muscle area in  $\text{mm}^2$ ) was determined on cross-sections spanning the entire muscle segment and averaging these numbers for each segment and for each mouse.

*Quantification of differentiation:* For studies with GFP<sup>+</sup> mouse cells, a similar method was used as for engraftment cell density (see above), however differentiation was determined only on serial cross-sections from the frozen 2 mm segment stained with red fluorescence for cell-type specific markers (CD31 for EC and  $\alpha$ -SMA for SMC). Differentiation was determined by co-localization with green fluorescence by confocal microscopy. For studies with human cells, we determined co-localization by double staining for FITC-conjugated human-specific vimentin and red fluorescence stainings for cell-type specific markers (CD31 for EC and  $\alpha$ -SMA for SMC). Differentiation was expressed as the number of yellow cells (in which green co-localized with the red cell-type specific marker marker), relative to the total number of cells found in the graft and averaged for all cross-sections.

*Quantification of other histological parameters:* For each muscle, all measurements were done on cross-sections chosen with regular intervals spanning a 2 mm muscle segment. For most of the parameters and when technically feasible ( $\alpha$ -SMA, necrosis and regeneration on H&E, desmin, CD45), entire cross-sections were evaluated on lower power field images. For the remainder of the parameters (capillary density on CD31, N-CAM, fibrosis on Sirius Red), adequate analysis required higher resolution, in which case several (usually 3 per cross-section) randomly chosen higher power fields covering a large part of each cross-section were analyzed. All parameters were expressed as % positive area per cross-sectional muscle area.

*Evaluation of fusion in vivo:* Fusion was analyzed by confocal microscopy on cross-sections, stained with laminin conjugated to a red fluorescence signal and counterstained with Topro to

allocate nuclei to muscle fibers (which are within the laminin border) and distinguish them from nuclei of satellite cells and inflammatory cells (which are outside the laminin border). To look for fusion chimeras in the cross-sections, we screened for the presence of muscle cells that had GFP<sup>+</sup> cytoplasm (contributed by the MAPC) and GFP<sup>-</sup> nuclei (contributed by a host cell) or fibers in which MAPC-derived GFP<sup>+</sup> and host-derived GFP<sup>-</sup> nuclei could be found in the same fiber.

***RNA isolation, Q-RT-PCR, cytokine production, cell proliferation/differentiation assays***

RNA isolation and Q-RT-PCR: Total RNA from undifferentiated and differentiated cells was extracted using the RNAeasy minikit (Qiagen). mRNA was reverse transcribed using Superscript II Reverse Transcriptase (Invitrogen) and cDNA underwent 40 rounds of amplification (ABI PRISM 7700, Perkin Elmer/Applied Biosystems) as follows: 40 cycles of a two step PCR (95°C for 15", 60°C for 60") after initial denaturation (95°C for 10') with 1µl of cDNA template, 1µl of primer mix and 1x TaqMan SYBR Green Universal Mix PCR reaction buffer (Applied Biosystems). Primers used for amplification are shown in supplementary Table S3. mRNA levels were normalized using *GAPDH* as housekeeping gene.

Cytokine production assays: To assess cytokine production of mMAPC-U, cells were plated in triplicate in cytokine-free and low serum expansion media and supernatant was collected 60 hours later and frozen. mBMC were plated in DMEM supplemented with 10% serum. ELISA kits were from R&D Systems and the procedure was performed according to the manufacturer's recommendations.

Cell proliferation assays: For proliferation assays, MS-I EC, C2C12 myoblasts (both from ATCC), and RaoSMC (Cell Applications) were plated in triplicate and 2 hours later, 75% of the media was replaced with conditioned media in half of the wells and in the other half, 75% of the media was replaced with unconditioned media (that had been incubated for 60 hours in the absence of cells). In order to avoid artifacts due to serum depletion during the 60-hour incubation, serum levels were replenished. 72 hours later, cells were harvested by trypsinization and counted.

Cell differentiation/fusion assay: To study fusion in vitro, 4x10<sup>4</sup> MAPC-U were co-cultured with 4x10<sup>4</sup> PKH26-labeled C2C12 cells under proliferating conditions (DMEM with 10% FBS). From day 4 to 10, 50% of the media was replaced with serum-free media to induce differentiation. Cultures were screened by confocal microscopy.

***Statistical analysis***

Data, expressed as mean $\pm$ SEM, when comparing two groups, were analyzed by using the unpaired Student's *t*-test. Comparisons among 4 groups were analyzed by ANOVA. A Kolmogorov-Smirnov test was used to verify that the data had a Gaussian distribution, which justified the use of a parametric test. InStat3.0a software was used for statistical analyses and differences were considered statistically significant when  $P < 0.05$ .

**II. Supplementary movie M1**

Movie showing a tail-suspension test in which the mobility of the hind limbs was observed for 10 seconds and compared between mMAPC-U-treated and vehicle-injected mice. Note the more vigorous movement of the hind legs (most notably the cell-injected left leg) by the mMAPC-U-treated mouse (on the left) and the more lethargic behavior of the vehicle-injected mouse (on the right). This test was performed 9 days after ligation and was highly reproducible in other mouse pairs subjected to this test (not shown).

### III. Supplementary tables

**Table S1: Overview of clinical studies using cell transplantation in PVD patients.**

<i>Reference</i>	<i>Patients</i>	<i>Cell populations</i>	<i>Transplantation method</i>
Hernández et al. (13)	N=12; all CLI	BMMNC (density gradient or cell separator)	i.m. (gastrocnemius)
Lenk et al. (14)	N=7; all CLI	CPC (ex vivo expanded)	i.a. (femoral artery)
Bartsch et al. (15)	N=10; all CLI	BMMNC (density gradient)	i.m. (gastrocnemius and quadriceps) and i.a. (femoral artery)
Miyamoto et al. (16)*	N=8; all TAO	BMMNC (cell separator)	i.m. (gastrocnemius, soleus)
Durdu et al. (17)	N=28; all CLI	BMMNC (cell separator)	i.m. (gastrocnemius, intermetatarsal region)
Saigawa et al. (18)	N=8; all AO	BMMNC (cell separator)	i.m. (location not specified)
Huang et al. (19)	N=28; all CLI	PBMNC (G-CSF mobilized, cell separator)	i.m. (thigh muscle)
Ishida et al. (20)	N=6; 5 TAO, 1 AO	PBMNC (G-CSF mobilized, cell separator)	i.m. (location not specified)
Higashi et al. (21)	N=7; all CLI	BMMNC (cell separator)	i.m. (gastrocnemius)
Tateishi-Yuyama et al. (22)	N=54; all CLI	BMMNC or PBMNC (cell separator)	i.m. (gastrocnemius)
Huang et al. (23)	N=5; all AO	PBMNC (G-CSF mobilized, cell separator)	i.m. (lower limb muscle)
Yang et al. (24)	N=62; all CLI	PBMNC (G-CSF mobilized)	i.m. (lower extremity + foot)
Miyamoto et al. (25)	N=19; all CLI	BMMNC combined with platelets	i.m. (location not specified)
Nizankowski et al. (26)	N=10; all CLI	BMMNC (cell separator)	i.m. (pedal and tibial region)
Gu et al. (27)	N=35; 5 IC, 30 CLI	BMMNC (G-CSF stimulated)	i.m., i.a. or a combination of both
Bartsch et al. (28)	N=1; CLI	BMMNC	i.m. and i.a. (combined)
Gu et al. (29)	N=22; half with 'mild', half with 'severe' ischemia	BMMNC	i.m. (location not specified)

\*4 out of 8 patients experienced negative effects in the long term after i.m. injection of BMMNC

*Abbreviations:* CLI: critical limb ischemia; IC: intermittent claudication; TAO: Thromboangiitis Obliterans; AO: Atherosclerosis Obliterans; BMMNC: bone marrow mononuclear cells; PBMNC: peripheral blood mononuclear cells; CPC: circulating progenitor cells

**Table S2: List of primary antibodies**

Antigen	Species	Supplier, catalogN°	Dilution	Label
GFP	Jellyfish	Clonotech	1:120	None
$\alpha$ -SMA	Mouse	DAKO, C-6198	1:200	Cy-3
CD31	Mouse	Pharmlingen, 557355	1:500	None
CD45	Mouse	Pharmlingen, 553076	1:500	None
BS-I lectin	Mouse	Sigma	1:100	Biotin
N-CAM	Mouse	Monosan	1:50	None
Desmin	Mouse	ICN, 10519	1:50	None
Vimentin	Human	DAKO	1:100	None
CD31	Human	DAKO	1:40	None
Desmin	human/mouse	DAKO	1:100	None
CD117	Mouse	Pharmlingen, 553354	1:200	FITC
CD19	Mouse	Pharmlingen, 550284	1:50	None
CD3	Mouse	Pharmlingen, 555273	1:50	None
Mac-3	Mouse	Pharmlingen, 553322	1:200	None
CD11c	Mouse	Pharmlingen, 550289	1:20	None
CD45	Mouse	Pharmlingen, 553076	1:100	None
VEGF	Mouse	Santa-Cruz, Sc-152	1:20	None
IGF-1	Mouse	Abcam, ab15320	1:4 (prediluted)	None
laminin	Mouse	Sigma, L9393	1:50	None

**Table S3: List of Q-RT-PCR primers**

Gene name	Primer sequence (5'-3')	User concentration
<i>Flt-1 (VEGFR-1)</i>	<b>F: TGGCCAGAGGCATGGAGT</b> <b>R: TCGCAAATCTTCACCACATTG</b>	<b>200 nM, detection: Sybr Green</b>
<i>PECAM (CD31)</i>	<b>F: GTCATGGCCATGGTCGAGTA</b> <b>R: CTCCTCGGCGATCTTGCTGAA</b>	
<i>VEC (VE-cadherin)</i>	<b>F: ATTGAGACAGACCCCAAACG</b> <b>R: TTCTGGTTTTCTGGCAGCTT</b>	
<i>EB2 (ephrin-B2)</i>	<b>F: ACAGGTGGGAGGTGACTGAC</b> <b>R: GCTGCGCTTTTTATTTCAG</b>	

Abbreviations: F: forward; R: reverse

#### IV. Legends to supplementary figures

##### Figure S1. Cell injection and assessment of contralateral engraftment and circulating cells

**A,B**, Injection procedure: Injection sites (3 for the adductor region (A) and 3 for the gastrocnemius muscle(B)) were equally spaced and selected as such in order to cover the majority of the muscle area.  $1.7 \times 10^5$  cells were delivered in each injection site. **C-E**, In vivo imaging revealed no GFP signal in vehicle-treated adductor (C) or contralateral adductor muscles (E) of mMAPC-U-injected animals, whereas the injected ('ipsilateral') adductor of the same mouse showed a bright GFP signal (D). All images were recorded 14 days post-transplantation. **F**, FACS dot-plot of a blood sample taken from an mMAPC-U-transplanted mouse 9 days after transplantation, revealing no circulating GFP<sup>+</sup> (X-axis) cells (lower right quadrant). The Y-axis represents the red fluorescent channel. Scale bars: 500  $\mu$ m (C-E).

##### Figure S2. In vitro and in vivo skeletal muscle differentiation: fusion or not?

**A**, Schematic representation of the co-culture assay of mMAPC-U with C2C12 myoblasts showing two potential mechanisms, direct differentiation (left) or fusion (right). **B-D**, Pictures showing a GFP<sup>+</sup> multi-nucleated myofiber (B), the same microscopic field stained with desmin (red; C) and the merged picture in (D). White arrowheads indicate the same fiber in all panels. **E-G**, Pictures showing a GFP<sup>+</sup> multi-nucleated myofiber (E), the same microscopic field showing PKH26-labeled C2C12 cells (red; F) and the merged picture in (G) revealing that the multi-nucleated fiber (indicated by white arrowheads in all panels) was not fused with C2C12 cells. **H-J**, Pictures showing GFP<sup>+</sup> MAPCs (H), the same microscopic field showing PKH26-labeled C2C12 cells (red; I) and the merged picture in (J) revealing that the multi-nucleated fiber (indicated by white and yellow arrowheads in all panels and delineated by white dashed lines) was fused (yellow arrowhead) with C2C12 cells. **K**, Schematic representation of the rationale used to study MAPC-U contribution to regenerating skeletal muscle (represented by cells with central nuclei) and eventually more differentiated fibers (represented by cells with lateral nuclei) in vivo, showing two options: direct differentiation (left), during which MAPC-U form new fibers by fusion amongst themselves (all nuclei are GFP<sup>+</sup>, i.e. green), or fusion (right), during which MAPC-U fuse with host myofibers, forming heterokaryons (containing GFP<sup>+</sup> (i.e. green) nuclei and host-derived GFP<sup>-</sup> (i.e. blue) nuclei). Whether these phenomena happen through a satellite cell ('S') intermediate remains to be determined. **L-N**, Confocal pictures showing muscle fibers in cross-section with laminin stained in red, MAPC-derived cells in green (GFP) and nuclei in blue (Topro), revealing that the regenerating green cell on the right with central GFP<sup>-</sup> (dark

blue) nucleus is the result of fusion (blue arrowhead in N). **O-Q**, Confocal pictures showing muscle fibers in transversal section with laminin stained in red, MAPC-derived cells in green (GFP) and nuclei in blue (Topro), revealing that the cell on the right is the result of fusion featuring one GFP<sup>-</sup> (blue nucleus; dark blue arrowheads in P,Q) and one GFP<sup>+</sup> nucleus (light blue arrowhead in Q). **R-T**, Confocal pictures showing muscle fibers in cross-section with laminin stained in red, MAPC-derived cells in green (GFP) and nuclei in blue (Topro), revealing that the green cell on the right with lateral GFP<sup>-</sup> (dark blue) nucleus is the result of fusion (dark blue arrowheads in S,T). Note the hybrid vessel (lumen indicated with white asterisk), containing a MAPC-derived (GFP<sup>+</sup> nucleus in R; light blue arrowhead in T) endothelial cell and a host-derived (GFP<sup>-</sup> nucleus in R; white arrowhead in T) endothelial cell. Scale bars: 40  $\mu\text{m}$  (B-D), 25  $\mu\text{m}$  (E-J), 15  $\mu\text{m}$  (L-Q) and 10  $\mu\text{m}$  (R-T).

### Figure S3. Characterization of mMAPC-derived endothelial progenitors

**A**, Bar graph representing in vitro endothelial gene expression (*VE-cadherin* or *VEC*, *CD31*, *Flt1* and arterial specific *ephrinB2* or *EB2*) until 14 days after exposure of mMAPC-U to VEGF<sub>165</sub>, analyzed by quantitative RT-PCR, expressed as fold increase versus undifferentiated cells. All experiments were done in quadruplicate and the graph shows mean fold increase  $\pm$  SEM. Note that the expression of EC markers still significantly increased beyond day 9, indicating that the cells were still not mature at this time point. \*:  $P < 0.05$  versus earlier time point. **B**, BS-I lectin staining (red) of GFP<sup>+</sup> (green) mMAPC-derived endothelial progenitors, 9 days after the start of differentiation, revealing that the majority of the cells was able to bind lectin, indicating homogenous differentiation. **C**, Similarly, the majority of the cells (green), after 9 days of differentiation, was able to take up AcLDL (red) after 4 hours incubation. **D**, Three-dimensional matrigel assay, showing organization of mMAPC-derived progenitors in tubes. Tube formation only occurred after a significant lagtime ( $\approx$  2 weeks), again suggesting that mMAPC EC-differentiated for 9 days are not fully mature, but rather endothelial precursors. Scale bars: 50  $\mu\text{m}$  (C), 100  $\mu\text{m}$  (B) and 500  $\mu\text{m}$  (D).

### Figure S4. Regional and temporal parameter changes recorded with MRSI

**A**, Graph illustrating regional changes in energetic status by magnetic resonance spectroscopy/imaging (MRSI) in the hind limb of a mouse 1 day after ligation of the femoral artery. Recordings were done at five different levels of the hind limb (v1, v2, v3, v4 and v5), as indicated in the anatomic image (left). The bar graphs display the PCr/P<sub>i</sub> ratios (middle) and the PCr/ $\gamma$ -ATP ratios (right) at the 5 levels. Note that the ratios decrease (i.e. energetic status

becomes worse) as we follow the limb further down to the foot. **B**, Spectra illustrating temporal changes in energetic status in region v5 (the region most severely affected) detected by MRSI in the hind limb of a normal mouse ('sham'; left panel), a vehicle-treated mouse 1 day after ligation (middle panel; red line overlays the normal mouse curve), and a vehicle-treated mouse 9 days after ligation (right panel; red line overlays the normal mouse curve). Note the increase in  $P_i$  and simultaneous decrease in PCr on day 1, resulting in a lower PCr/ $P_i$  ratio and a lower PCr/ $\gamma$ -ATP ratio, and thus a significantly lower sum of both parameters ( $\Sigma=23$  in sham versus  $\Sigma=4$  in day 1 vehicle). On day 9, PCr rises again, resulting in higher PCr/ $P_i$  and PCr/ $\gamma$ -ATP ratios, with the sum of both parameters being higher again ( $\Sigma=12$  on day 9 versus  $\Sigma=4$  on day 1).

**Figure S5. Characterization of inflammatory infiltrates in mBMC-transplanted gastrocnemius muscles**

**A**, Cross-section of a gastrocnemius muscle of an mBMC-treated mouse massively infiltrated by inflammatory clusters (indicated by asterisks). Small square corresponds to the area shown in higher magnification in B-F. **B-F**, Serial cross-sections of gastrocnemius muscle of an mBMC-treated mouse focussing on one of the inflammatory clusters, stained with an anti-GFP antibody (B), and a panel of inflammatory markers revealing that the majority of cells were T-cells (F) and dendritic cells (E), whereas macrophages (D) were less represented and B-cells (C) were absent from the clusters. A vessel is indicated as reference point with dashed black circles in B-F. Hematoxylin was used as nuclear counterstain in all panels. Scale bars: 50  $\mu\text{m}$  (B-F) and 500  $\mu\text{m}$  (A).

**Figure S6. mMAPC-U co-localize with VEGF and IGF-1 in vivo**

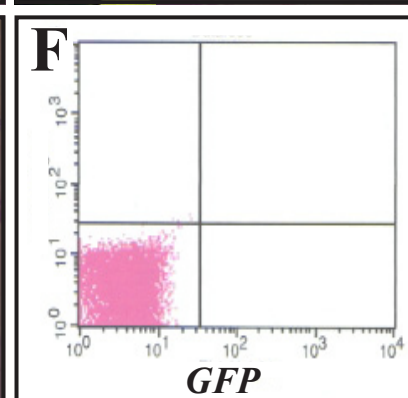
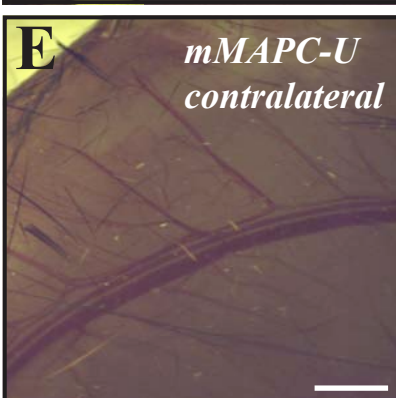
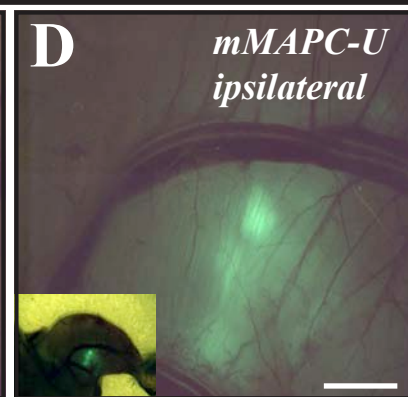
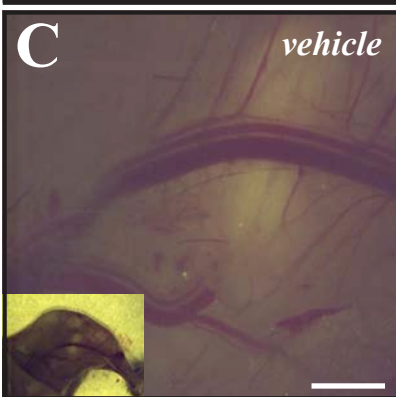
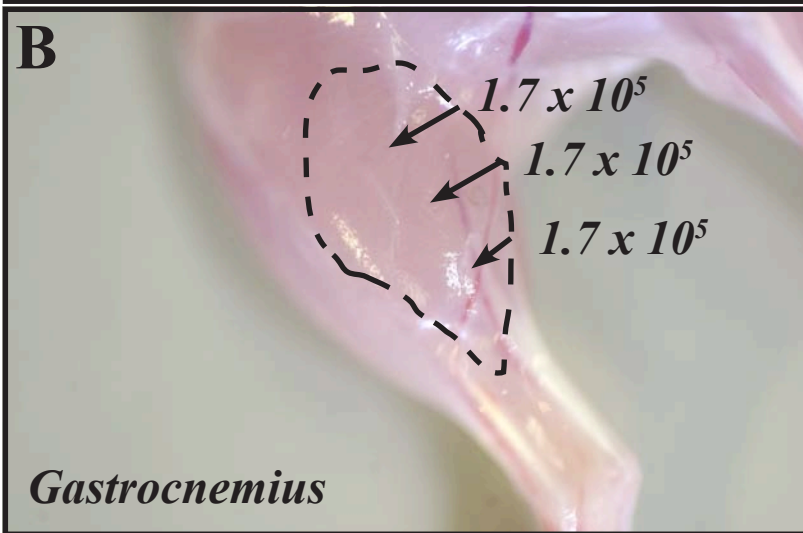
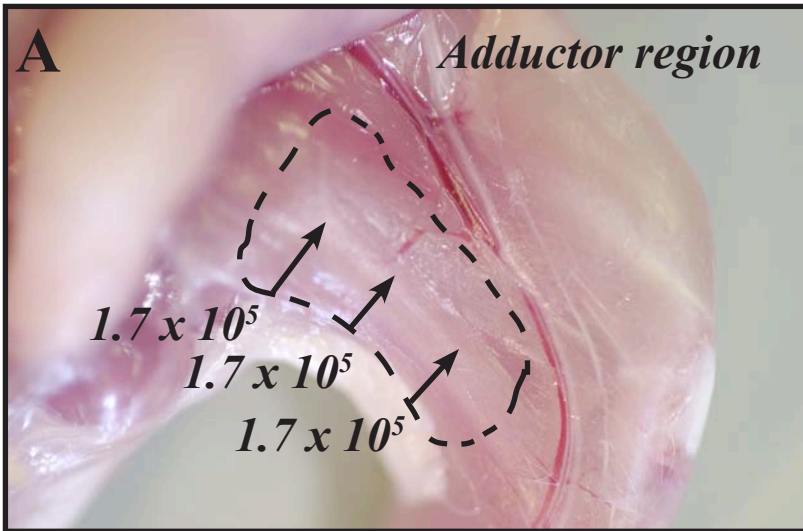
**A-C**, Cross-section through a gastrocnemius muscle of an mMAPC-U-treated mouse: the VEGF-signal (red in B,C) co-localizes (yellow in C) significantly with the transplanted cells (green in A,C). **D-G**, Serial cross-sections through an adductor muscle (D,E) and a gastrocnemius muscle (F,G) of an mMAPC-U-treated mouse, stained with anti-GFP (D,F) or anti-IGF-1 (E,G) revealing co-localization of the IGF-1 protein with the engrafted cells. Corresponding regions in the serial sections are delineated by dashed lines. Note that the IGF-1 (arrowheads in G) in the gastrocnemius muscle is surrounding regenerating fibers (with central nuclei). Scale bars: 45  $\mu\text{m}$  (D-G) and 150  $\mu\text{m}$  (A-C).

## V. References in supplement

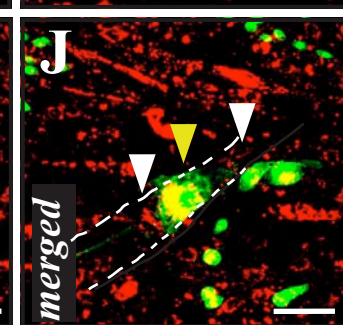
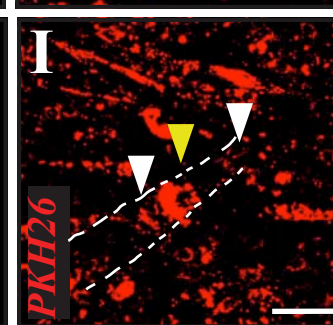
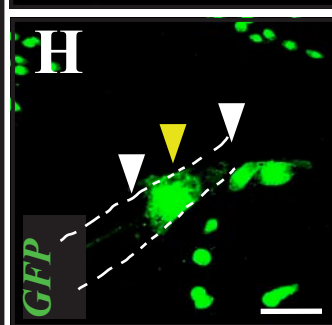
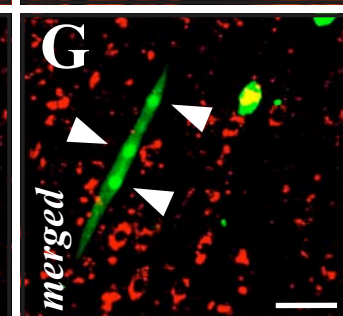
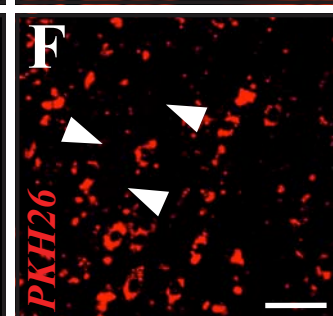
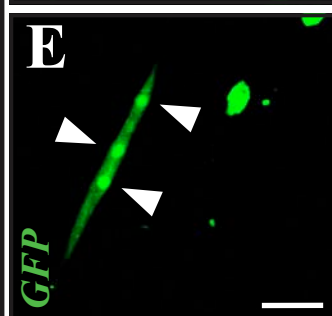
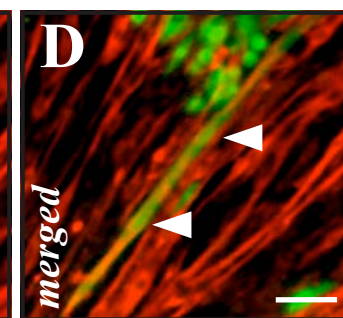
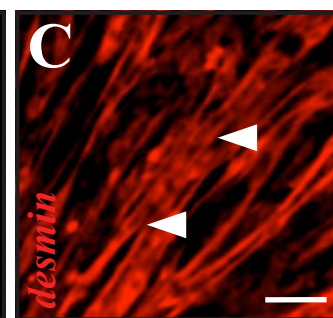
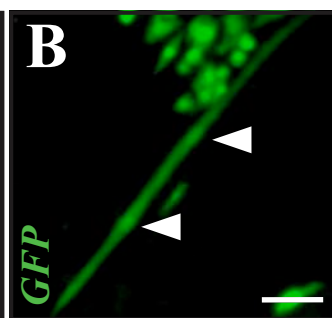
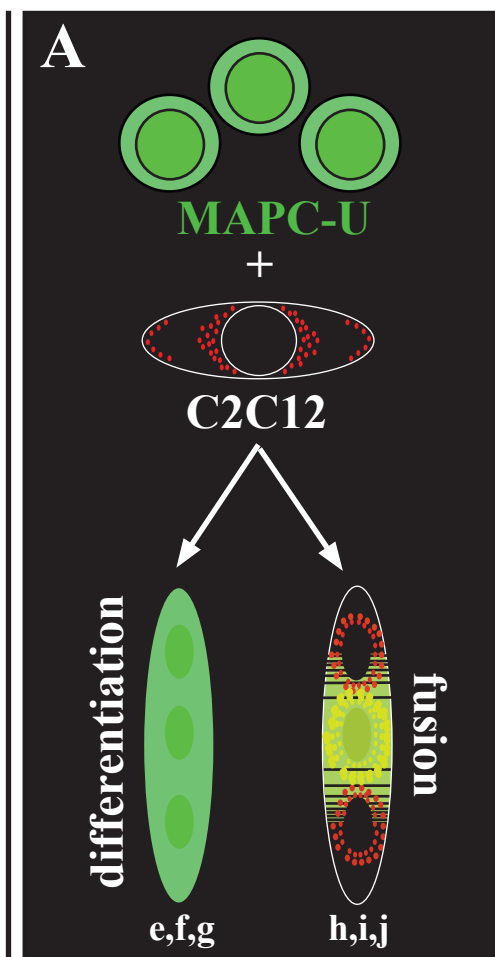
1. Ulloa-Montoya, F., Kidder, B.L., Pauwelyn, K.A., Chase, L.G., Luttun, A., Crabbe, A., Geraerts, M., Sharov, A.A., Piao, Y., Ko, M.S., et al. 2007. Comparative transcriptome analysis of embryonic and adult stem cells with extended and limited differentiation capacity. *Genome Biol* 8:R163.
2. Aranguren, X.L., Luttun, A., Clavel, C., Moreno, C., Abizanda, G., Barajas, M.A., Pelacho, B., Uriz, M., Arana, M., Echavarri, A., et al. 2007. In vitro and in vivo arterial differentiation of human multipotent adult progenitor cells. *Blood* 109:2634-2642.
3. Reyes, M., Dudek, A., Jahagirdar, B., Koodie, L., Marker, P.H., and Verfaillie, C.M. 2002. Origin of endothelial progenitors in human postnatal bone marrow. *J Clin Invest* 109:337-346.
4. Ross, J.J., Hong, Z., Willenbring, B., Zeng, L., Isenberg, B., Lee, E.H., Reyes, M., Keirstead, S.A., Weir, E.K., Tranquillo, R.T., et al. 2006. Cytokine-induced differentiation of multipotent adult progenitor cells into functional smooth muscle cells. *J Clin Invest* 116:3139-3149.
5. Couffinhal, T., Silver, M., Kearney, M., Sullivan, A., Witzensbichler, B., Magner, M., Annex, B., Peters, K., and Isner, J.M. 1999. Impaired collateral vessel development associated with reduced expression of vascular endothelial growth factor in ApoE<sup>-/-</sup> mice. *Circulation* 99:3188-3198.
6. Helisch, A., Wagner, S., Khan, N., Drinane, M., Wolfram, S., Heil, M., Ziegelhoeffer, T., Brandt, U., Pearlman, J.D., Swartz, H.M., et al. 2006. Impact of mouse strain differences in innate hindlimb collateral vasculature. *Arterioscler Thromb Vasc Biol* 26:520-526.
7. Masaki, I., Yonemitsu, Y., Yamashita, A., Sata, S., Tanii, M., Komori, K., Nakagawa, K., Hou, X., Nagai, Y., Hasegawa, M., et al. 2002. Angiogenic gene therapy for experimental critical limb ischemia: acceleration of limb loss by overexpression of vascular endothelial growth factor 165 but not of fibroblast growth factor-2. *Circ Res* 90:966-973.
8. Stabile, E., Kinnaird, T., la Sala, A., Hanson, S.K., Watkins, C., Campia, U., Shou, M., Zbinden, S., Fuchs, S., Kornfeld, H., et al. 2006. CD8<sup>+</sup> T lymphocytes regulate the arteriogenic response to ischemia by infiltrating the site of collateral vessel development and recruiting CD4<sup>+</sup> mononuclear cells through the expression of interleukin-16. *Circulation* 113:118-124.
9. Tolar, J., O'Shaughnessy M, J., Panoskaltsis-Mortari, A., McElmurry, R.T., Bell, S., Riddle, M., McIvor, R.S., Yant, S.R., Kay, M.A., Krause, D., et al. 2006. Host factors that impact the biodistribution and persistence of multipotent adult progenitor cells. *Blood* 107:4182-4188.
10. Seaman, W.E., Sleisenger, M., Eriksson, E., and Koo, G.C. 1987. Depletion of natural killer cells in mice by monoclonal antibody to NK-1.1. Reduction in host defense against malignancy without loss of cellular or humoral immunity. *J Immunol* 138:4539-4544.
11. Luttun, A., Tjwa, M., Moons, L., Wu, Y., Angelillo-Scherrer, A., Liao, F., Nagy, J.A., Hooper, A., Priller, J., De Klerck, B., et al. 2002. Revascularization of ischemic tissues by PlGF treatment, and inhibition of tumor angiogenesis, arthritis and atherosclerosis by anti-Flt1. *Nat Med* 8:831-840.

12. Ytrehus, K., Liu, Y., Tsuchida, A., Miura, T., Liu, G.S., Yang, X.M., Herbert, D., Cohen, M.V., and Downey, J.M. 1994. Rat and rabbit heart infarction: effects of anesthesia, perfusate, risk zone, and method of infarct sizing. *Am J Physiol* 267:H2383-2390.
13. Hernandez, P., Cortina, L., Artaza, H., Pol, N., Lam, R.M., Dorticos, E., Macias, C., Hernandez, C., Del Valle, L., Blanco, A., et al. 2006. Autologous bone-marrow mononuclear cell implantation in patients with severe lower limb ischaemia: A comparison of using blood cell separator and Ficoll density gradient centrifugation. *Atherosclerosis*.
14. Lenk, K., Adams, V., Lurz, P., Erbs, S., Linke, A., Gielen, S., Schmidt, A., Scheinert, D., Biamino, G., Emmrich, F., et al. 2005. Therapeutical potential of blood-derived progenitor cells in patients with peripheral arterial occlusive disease and critical limb ischaemia. *Eur Heart J* 26:1903-1909.
15. Bartsch, T., Falke, T., Brehm, M., Zeus, T., Kogler, G., Wernet, P., and Strauer, B.E. 2006. [Intra-arterial and intramuscular transplantation of adult, autologous bone marrow stem cells. Novel treatment for therapy-refractory peripheral arterial occlusive disease]. *Dtsch Med Wochenschr* 131:79-83.
16. Miyamoto, K., Nishigami, K., Nagaya, N., Akutsu, K., Chiku, M., Kamei, M., Soma, T., Miyata, S., Higashi, M., Tanaka, R., et al. 2006. Unblinded pilot study of autologous transplantation of bone marrow mononuclear cells in patients with thromboangiitis obliterans. *Circulation* 114:2679-2684.
17. Durdu, S., Akar, A.R., Arat, M., Sancak, T., Eren, N.T., and Ozyurda, U. 2006. Autologous bone-marrow mononuclear cell implantation for patients with Rutherford grade II-III thromboangiitis obliterans. *J Vasc Surg* 44:732-739.
18. Saigawa, T., Kato, K., Ozawa, T., Toba, K., Makiyama, Y., Minagawa, S., Hashimoto, S., Furukawa, T., Nakamura, Y., Hanawa, H., et al. 2004. Clinical application of bone marrow implantation in patients with arteriosclerosis obliterans, and the association between efficacy and the number of implanted bone marrow cells. *Circ J* 68:1189-1193.
19. Huang, P., Li, S., Han, M., Xiao, Z., Yang, R., and Han, Z.C. 2005. Autologous transplantation of granulocyte colony-stimulating factor-mobilized peripheral blood mononuclear cells improves critical limb ischemia in diabetes. *Diabetes Care* 28:2155-2160.
20. Ishida, A., Ohya, Y., Sakuda, H., Ohshiro, K., Higashiuesato, Y., Nakaema, M., Matsubara, S., Yakabi, S., Kakihana, A., Ueda, M., et al. 2005. Autologous peripheral blood mononuclear cell implantation for patients with peripheral arterial disease improves limb ischemia. *Circ J* 69:1260-1265.
21. Higashi, Y., Kimura, M., Hara, K., Noma, K., Jitsuiki, D., Nakagawa, K., Oshima, T., Chayama, K., Sueda, T., Goto, C., et al. 2004. Autologous bone-marrow mononuclear cell implantation improves endothelium-dependent vasodilation in patients with limb ischemia. *Circulation* 109:1215-1218.
22. Tateishi-Yuyama, E., Matsubara, H., Murohara, T., Ikeda, U., Shintani, S., Masaki, H., Amano, K., Kishimoto, Y., Yoshimoto, K., Akashi, H., et al. 2002. Therapeutic angiogenesis for patients with limb ischaemia by autologous transplantation of bone-marrow cells: a pilot study and a randomised controlled trial. *Lancet* 360:427-435.
23. Huang, P.P., Li, S.Z., Han, M.Z., Xiao, Z.J., Yang, R.C., Qiu, L.G., and Han, Z.C. 2004. Autologous transplantation of peripheral blood stem cells as an effective therapeutic

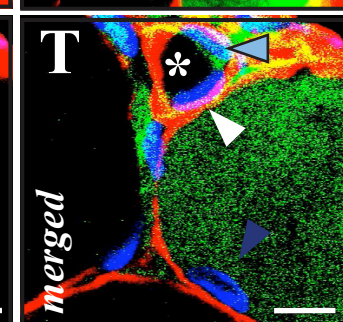
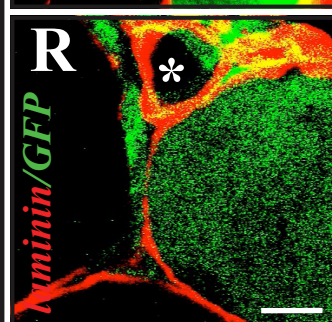
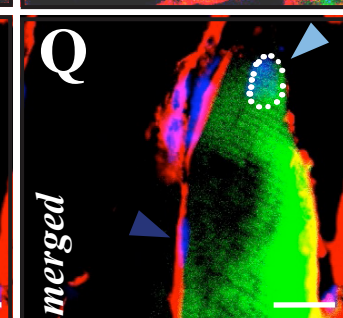
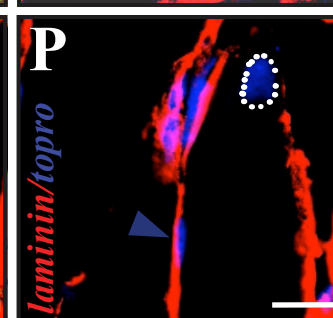
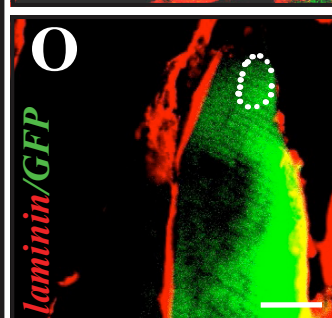
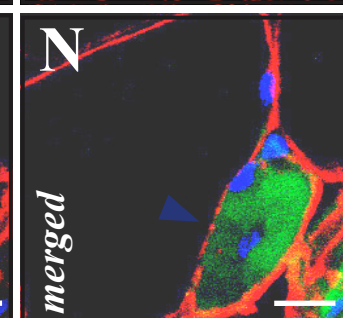
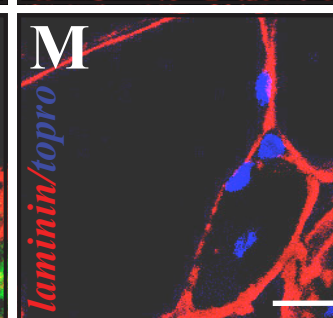
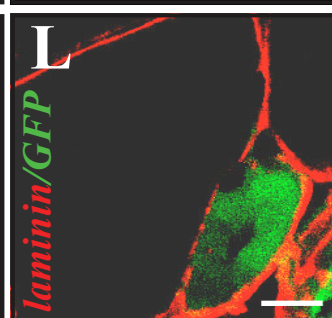
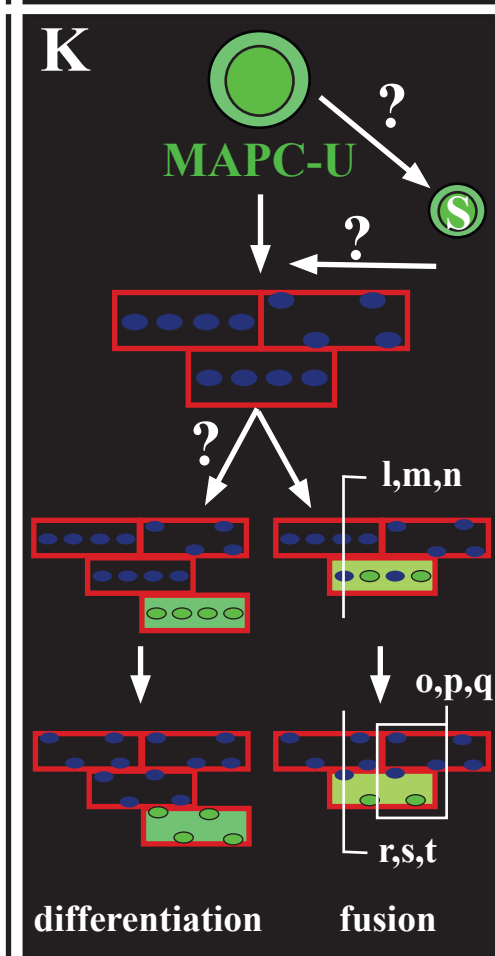
- approach for severe arteriosclerosis obliterans of lower extremities. *Thromb Haemost* 91:606-609.
24. Yang, X.F., Wu, Y.X., Wang, H.M., Xu, Y.F., Lu, X., Zhang, Y.B., Wang, F., and Zhang, Y. 2005. [Autologous peripheral blood stem cells transplantation in treatment of 62 cases of lower extremity ischemic disorder.]. *Zhonghua Nei Ke Za Zhi* 44:95-98.
  25. Miyamoto, M., Yasutake, M., Takano, H., Takagi, H., Takagi, G., Mizuno, H., Kumita, S., and Takano, T. 2004. Therapeutic angiogenesis by autologous bone marrow cell implantation for refractory chronic peripheral arterial disease using assessment of neovascularization by <sup>99m</sup>Tc-tetrofosmin (TF) perfusion scintigraphy. *Cell Transplant* 13:429-437.
  26. Nizankowski, R., Petriczek, T., Skotnicki, A., and Szczeklik, A. 2005. The treatment of advanced chronic lower limb ischaemia with marrow stem cell autotransplantation. *Kardiol Pol* 63:351-360; discussion 361.
  27. Gu, Y., Zhang, J., and Qi, L. 2006. [A clinical study on implantation of autologous bone marrow mononuclear cells after bone marrow stimulation for treatment of lower limb ischemia]. *Zhongguo Xiu Fu Chong Jian Wai Ke Za Zhi* 20:1017-1020.
  28. Bartsch, T., Falke, T., Brehm, M., Zeus, T., Kogler, G., Wernet, P., and Strauer, B.E. 2006. [Transplantation of autologous adult bone marrow stem cells in patients with severe peripheral arterial occlusion disease]. *Med Klin (Munich)* 101 Suppl 1:195-197.
  29. Gu, Y., Zhang, J., and Qi, L. 2006. [Effective autologous bone marrow stem cell dosage for treatment of severe lower limb ischemia]. *Zhongguo Xiu Fu Chong Jian Wai Ke Za Zhi* 20:504-506.

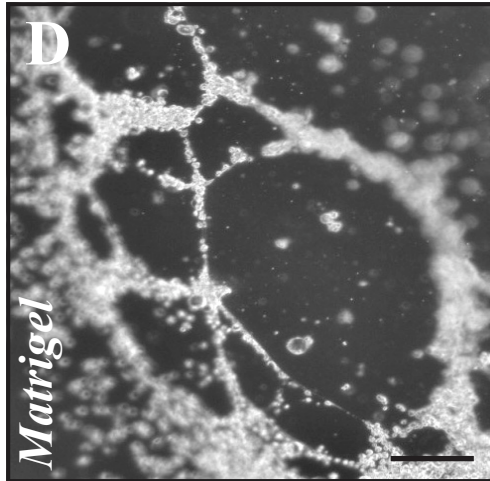
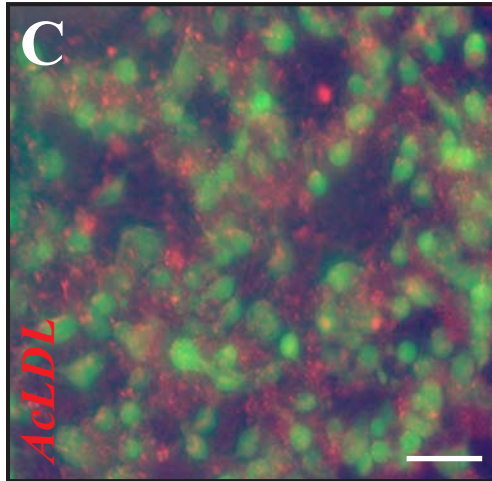
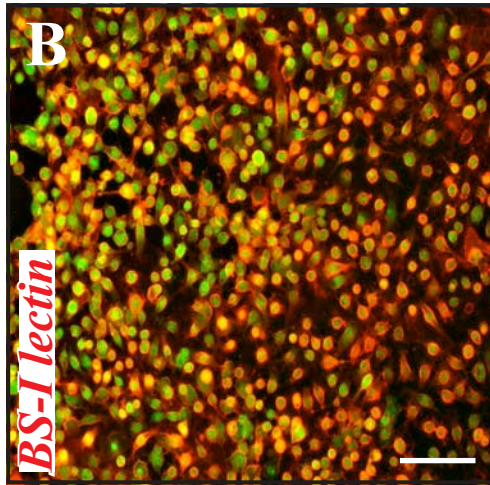
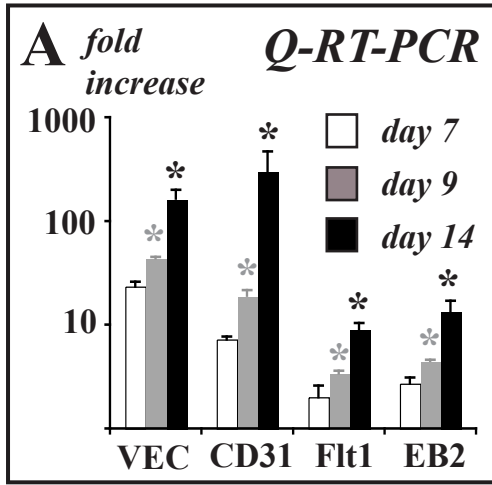


*in vitro*



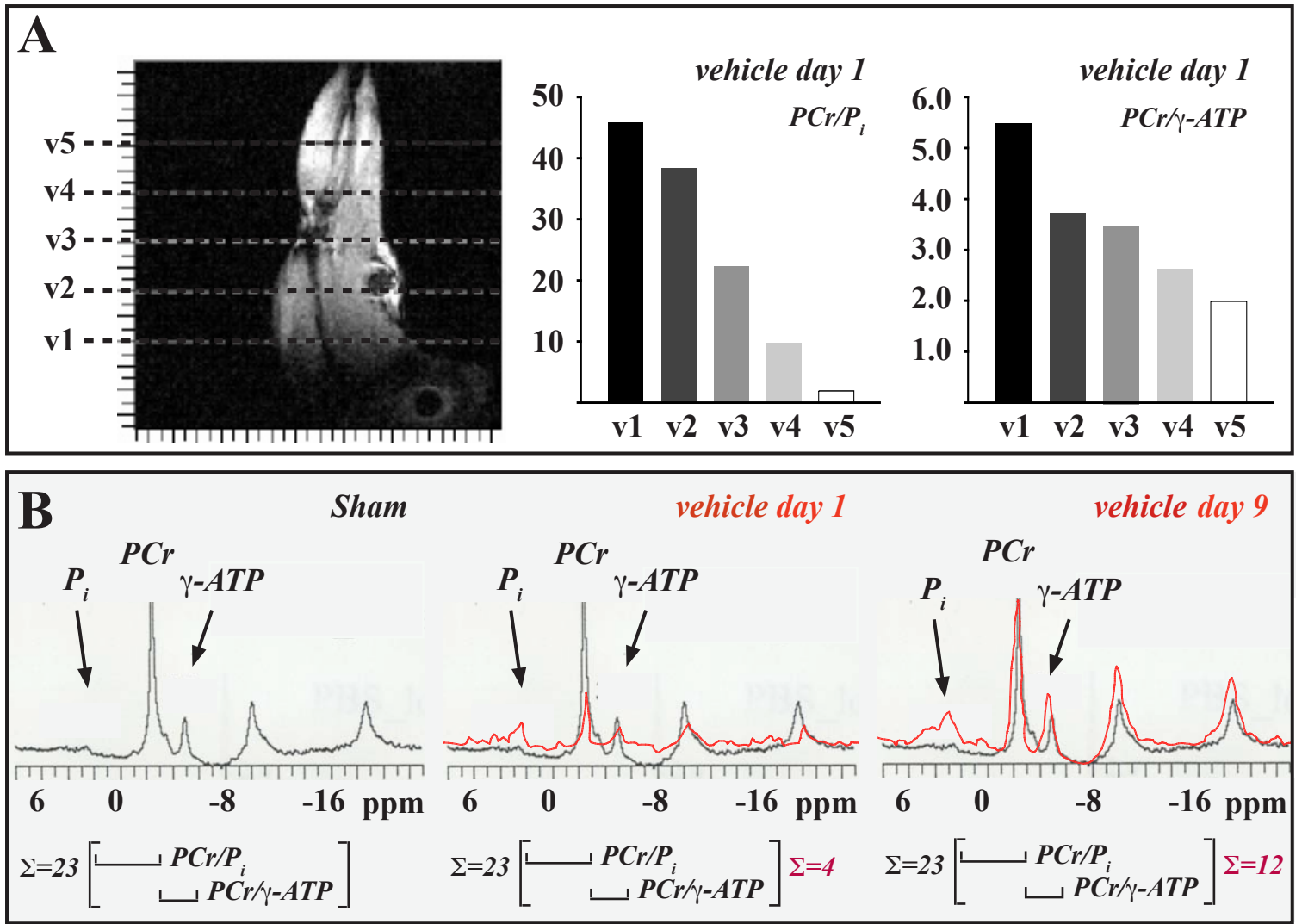
*in vivo*





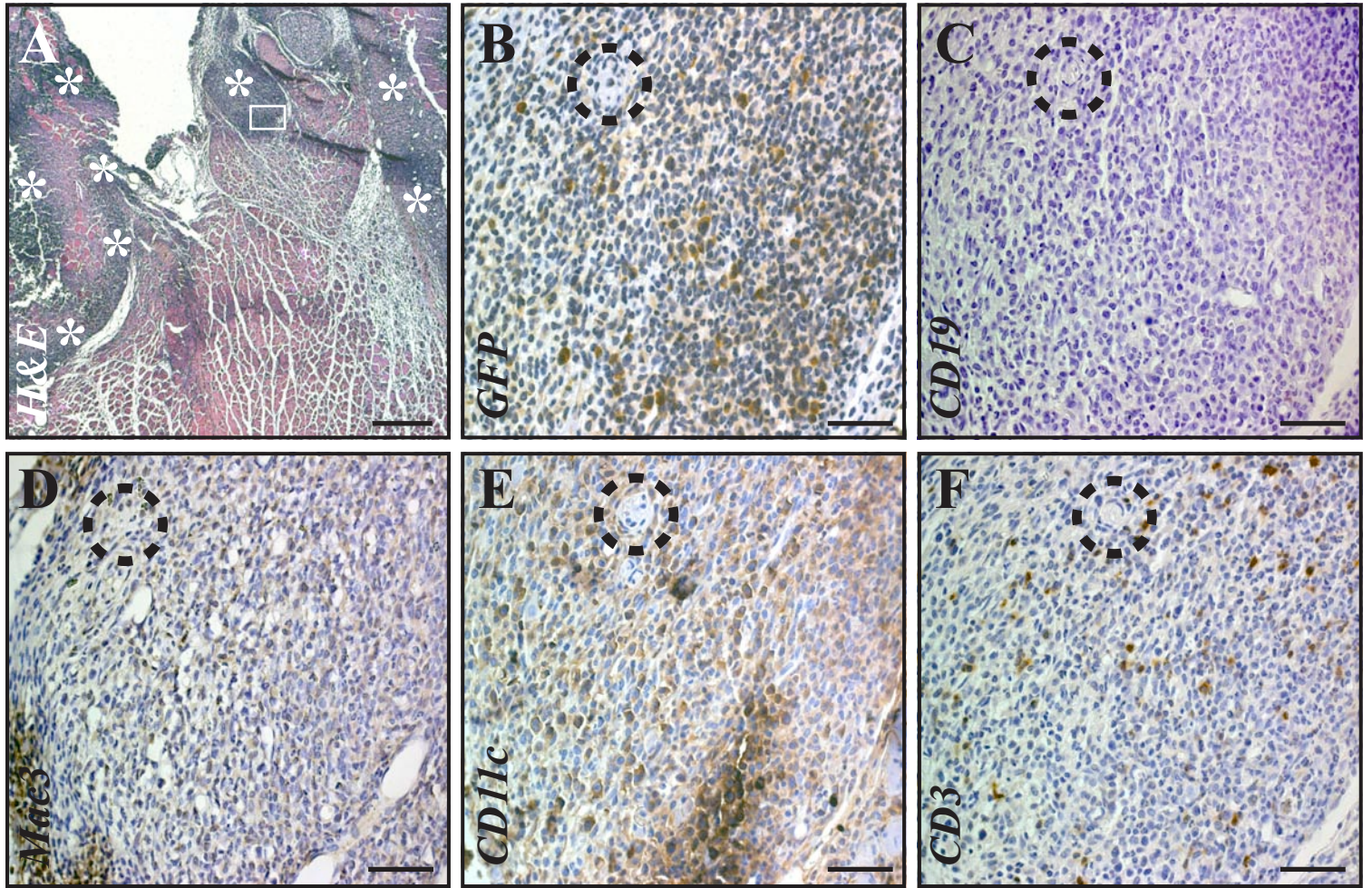
*Aranguren X. et al.*

*Figure S3*



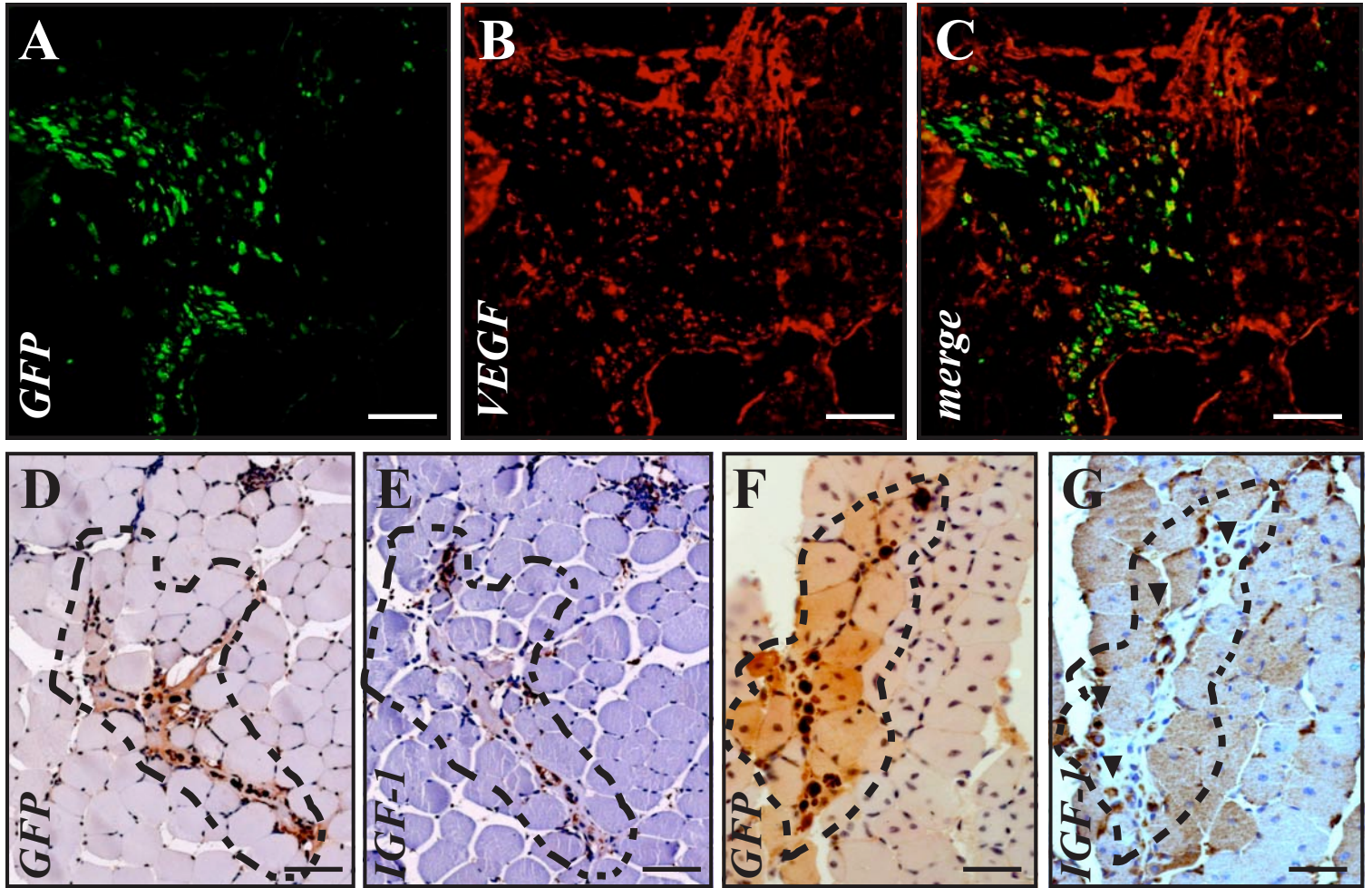
Aranguren X. et al.

Figure S4



*Aranguren X. et al.*

*Figure S5*



*Aranguren X. et al.*

*Figure S6*